Title: Vascular features, sucrose transport and Sucrose Synthase activity contribute to the differential source-sink relationship between a cultivated and a wild rice

Jyotirmaya Mathan, Anuradha Singh, Aashish Ranjan*
National Institute of Plant Genome Research, Aruna Asaf Ali Marg, New Delhi-110067, India.

***Correspondence**
Aashish Ranjan
National Institute of Plant Genome Research
Aruna Asaf Ali Marg
New Delhi – 110067, India
e-mail: aranjan@nipgr.ac.in

Running Head: Source-sink relationship in rice

Word Count: 6,992

Number of Figures: 7

Summary

The source-sink relationship is key to the overall crop performance in terms of biomass and grain yield. Detailed understanding of the factors that determine source-sink dynamics, such as developmental and physiological features of source and sink tissues, photoassimilate partitioning from source to sink tissues, and metabolic status of the tissues, is imperative for optimization of crop performance. We investigated the differences in the source-sink relationship between a cultivated rice variety *Oryza sativa* cv. Nipponbare and a wild rice *Oryza australiensis* that show striking differences in biomass and grain yield traits. The wild rice, accumulating higher biomass, was not only photosynthetically efficient but also had efficient phloem loading and sucrose export from leaves. However, sucrose was not efficiently mobilized to panicle due to fewer number of smaller vascular bundles at the panicle base as well as lower expression of *OsSWEET*s and *OsSUT1* in developing spikelets of *O. australiensis* compared to Nipponbare. High cleavage activity of Sucrose Synthase followed by higher expression of Cellulose Synthase genes in the wild rice stem efficiently utilized photosynthates for the synthesis of structural carbohydrates, resulting in high biomass. In contrast, the source-sink relationship favored high grain yield in Nipponbare via accumulation of transitory starch in the stem, due to higher expression of starch biosynthetic genes, to be mobilized to panicles with the onset of grain filling. Thus, vascular features and sucrose transporter functions together with functions of key sugar metabolic enzymes contributed to the variations in the source-sink relationship between the selected cultivated and wild rice.

Keywords: Source-sink relationship; Photosynthesis; Sucrose transport; Vascular features; Starch; Structural carbohydrates; Sucrose synthase; Biomass; Grain yield

Introduction

Source-sink relationship is critical for determining overall growth and performance of crop plants (White *et al.*, 2016). Photosynthetic carbon assimilation in source leaves, sucrose transport through vasculature, type and strength of sink tissues, as well as metabolic status of the tissues are the key features that determine the source-sink dynamics of a plant. Photosynthetic leaves are the major source tissues of a plant, whereas types and efficiency of sink organs vary depending upon the growth stages and environmental conditions. For example, grains are primary sink in the reproductive stage of crop plants, while roots, stem/internodes, and growing leaves function as the sink in the vegetative stage. Natural genetic variation for differences in the source-sink dynamics, resulting in changes in biomass and yield, has been evident (Burnett *et al.*, 2016; White *et al.*, 2016; Fabre *et al.* 2020). Many of the wild relatives of rice accumulate high biomass with poor grain filling, whereas cultivated varieties produce higher grain yield (Sanchez *et al.*, 2013).

Leaf morphological and anatomical features along with photosynthesis per unit leaf area largely determine the source strength of a plant (Mathan *et al.*, 2016). Functions of the key carbohydrate metabolic enzymes, such as ADP-glucose pyrophosphorylase (AGPase), sucrose phosphate synthase (SPS), sucrose phosphate phosphatase (SPP) and Sucrose synthase (SUS), are known to be key determinants of the metabolic status of source leaves (Osorio *et al.*, 2014; Ruan, 2014). Similarly, the capacity to utilize photosynthates efficiently largely determines the sink strength. Sink size, influenced by tiller number, spikelet number per panicle, and seed size; and sink activity, determined by functions of various metabolic enzymes such as cell wall invertase (cwINV) and sucrose synthase (SUS), dictate the photosynthates utilization at a sink organ (Smith *et al.*, 2018; Stein and Granot, 2019). Photosynthates are primarily partitioned from source leaves to different sink tissues in the form of sucrose via phloem with the aid of SWEET and SUT transporters (Braun, 2012; Chen *et al.*, 2012; Julius *et al.*, 2017). Mutations or overexpression of genes encoding sucrose transporters affect plant yield and biomass via modulation of source-sink dynamics (Scofield *et al.*, 2002; Chen *et al.*, 2012; Yang *et al.*, 2018). Besides the sucrose transporter functions, vascular features not only determine the rate of sucrose export from leaf tissues to phloem sap but also control mobilization of photosynthates to the panicles at the reproductive stage (Qi *et al.*, 2008; Fujita *et al.*, 2013; Sack and Scoffoni, 2013).

Photosynthates assimilated in leaves are either used to meet immediate cellular needs or mobilized into different sinks. Starch stored in leaves during the day, over and above the immediate utilization and transport of photosynthates, is degraded during the night to be transported to different sink organs for growth (Smith and Stitt, 2007; Chen *et al.*, 2012). Mutants defective in sucrose transport, usually, accumulate starch in leaves at the end of the night, limiting plant growth (Chen *et al.*, 2012). The utilization and storage of sugars are regulated diurnally as well as developmentally. Stem serves as the main storage organ for carbohydrates in crop plants, including rice, during vegetative growth. Sucrose, after getting unloaded into the stem, could possibly be converted to different non-structural carbohydrates (NSCs), such as glucose, fructose, and starch. Starch is reported to be the major storage

form in rice stem during the vegetative stage, which is mobilized to developing grains with the onset of the reproductive stage, contributing up to half of the final grain yield (Wang *et al.*, 2017). A portion of the photosynthates is also used as a structural component of the cell wall for the growth and development of new organs as well as elongation and thickening of existing organs. High biomass accumulation is usually associated with accumulation of cellulose and other structural carbohydrates in crop plants, with cellulose alone contributing around 25-50% of plant biomass (Haigler *et al.*, 2001). Thus, the balance of structural and non-structural carbohydrates derived from the sucrose in the stem is critical for determining biomass and grain yield in cereal crops.

Sucrose, after reaching to stem, is hydrolysed by two classes of enzymes, Invertases (INV) and Sucrose Synthase (SUS). Invertases cleave sucrose into glucose and fructose, while Sucrose Synthase (SUS) reversibly catalyses the formation of UDP-glucose and fructose. The UDP-glucose, generated by the cleavage activity of SUS, is used as a precursor for cellulose synthesis. Further, UDP-glucose can be converted to ADP-glucose for usage in starch synthesis, making SUS a key enzyme for biomass and grain yield (Smith *et al.*, 2012; Ruan, 2014; Stein and Granot, 2019). The functions of SUS is important for phloem loading and unloading as well as for determining sink strength (Smith *et al.*, 2012; Fan *et al.*, 2017; Yao *et al.*, 2020). Among the seven genes encoding SUS enzymes in rice, *OsSUS1* and *OsSUS3* contribute to seed starch biosynthesis (Cho *et al.*, 2011). Higher expression of *OsSUS3* also led to increased levels of structural carbohydrates, cellulose and hemicellulose, in rice (Fan *et al.*, 2017). *OsSUS1* is highly expressed in rice internodes, with a strong correlation with the expression pattern of genes encoding Cellulose Synthase, *OsCES4*, *OsCES7*, and *OsCES9* (Hirose *et al.*, 2008; Guevara *et al.*, 2014). Among Cellulose Synthase enzymes, OsCES4, OsCES7, and OsCES9 have been reported to function in secondary cell wall formation (Tanaka *et al.*, 2003; Wang *et al.*, 2016). Thus, functions of enzymes, such as INV, SUS and CES, are important for determining source-sink dynamics for biomass and grain yield.

Despite the key importance of sucrose partitioning and metabolism in determining source-sink relationship, this aspect is largely unexplored for optimization of grain yield and biomass in rice. Cultivated rice varieties and their wild relatives, with striking differences in yield and biomass traits, provide an excellent system to investigate the mechanistic basis of the source-sink relationship. We investigated the limitations related to sucrose transport and metabolism for grain yield in wild rice *O. australiensis*, resulting in higher biomass, compared to the cultivated variety *O. sativa* cv. Nipponbare. We report higher accumulation of structural carbohydrates, such as cellulose and hemicellulose, in the wild rice due to higher SUS cleavage activity together with higher expression of genes encoding Cellulose Synthases. Cultivated rice, in contrast, accumulated more starch in stem due to higher expression of genes encoding starch biosynthesis enzymes. We also establish the contribution of sucrose transporter functions and vascular features towards impaired mobilization of photosynthates to *O. australiensis* panicles.

Results

Biomass and grain yield differences among the selected wild and cultivated rice accessions

We initiated the study with two cultivated rice varieties, *Oryza sativa* ssp. *japonica* cv. Nipponbare and *Oryza sativa* ssp. *indica* cv. IR 64, and three wild relatives of rice, *Oryza rufipogon*, *Oryza latifolia,* and *Oryza australiensis* that show remarkable variations in overall growth and architectural features at both vegetative and reproductive stage (Figure 1a). All the selected wild rice species grew taller compared to the two cultivated varieties (Figure 1b). Among all the accessions, *O. sativa* cv. Nipponbare produced lowest number of total leaves, while *O. rufipogon* showed the highest number of leaves per plant (Figure 1c). Nipponbare showed a significantly lower number of leaves compared to all the selected wild species. In addition, Nipponbare also showed significantly lower tiller number per plant compared to all the selected accessions (Figure S1b). Selected wild rice species showed wider leaves compared to the cultivated varieties, with *O. latifolia* showing widest leaves (Figure 1d). We, then, quantified number and length of internodes in the main stem, as internodes are important contributors to the biomass of a plant. Cultivated rice varieties had fewer, smaller, and slender internodes in the main stem compared to the wild accessions (Figures 1e and S1a,c). In addition, stem width and circumference were also lower for Nipponbare and IR 64 compared to all selected wild species (Figures S1c,d). Thus, plant architectural traits, such as height, branching, and internode features, as well as leaf traits attributed to high biomass of the selected wild rice. Consistent with this, the selected wild rice also showed higher fresh and dry weight compared to the cultivated varieties. (Figures 1f,g).

We, then, quantified seed traits of the selected cultivated and wild rice. The cultivated rice varieties produced higher number of spikelets per panicle as well as higher seed weight compared to the wild relatives (Figures 1h,i). Higher seed weight of cultivated rice varieties resulted due to longer and wider grains compared to the wild species (Figure S1e,f). Principal Component analysis for all the quantified biomass and seed traits showed a clear separation of wild and cultivated genotypes (Figure S2). Taken together, these results confirmed the higher biomass accumulation at the expanse of grain yield in the selected wild rice compared to the cultivated varieties. Wild rice *O. australiensis* had higher phenotypic value for all the traits contributing to biomass, including tiller number, compared to Nipponbare. Therefore, we investigated the source strength, sink features, sucrose translocation as well as the fate of the photosynthates towards biomass and yield using representative wild rice and cultivated variety, *O. sativa* cv. Nipponbare and *O. australiensis*, respectively.

Comparison of source efficiency and photosynthates utilization

In order to compare source efficiency of the two selected accessions, we quantified leaf photosynthesis rate and related physiological traits as well as soluble sugars/non-structural carbohydrates (NSCs) content in leaves of the two accessions. A significant difference in the leaf photosynthesis rate *A* was observed between the two species at booting, and milk- and dough-stage of

grain filling. Both the species showed increasing trend of leaf photosynthesis from booting to milk stage, followed by reduction at the dough stage of grain filling (Figure S3a). The higher photosynthesis in *O. australiensis* at the three stages were also associated with higher g_sH_2O and *Ci* compared to Nipponbare (Figure S3b,c). Next, we measured the different soluble sugars/NSCs, such as sucrose, fructose, glucose and starch, at the time of photosynthesis quantification in leaves at the milk stage of grain filling to evaluate the levels of primary carbon metabolites, the major outcome of photosynthesis. The abundance of all four NSCs were significantly higher in the leaves of *O. australiensis* than Nipponbare (Figure 2a,b). Interestingly, *O. australiensis* also accumulated higher levels of starch in leaves compared to Nipponbare, suggesting abundance of residual sugar in the wild rice that are converted to starch. In contrast, the starch content was found to be significantly lower in *O. australiensis* grains compared to Nipponbare, despite starch being the major reserve product of seeds (Figures 2c). Higher starch and soluble sugar content in *O. australiensis* leaf and lower starch levels in seed suggested possible bottlenecks in the mobilization of photosynthates to grains in the wild rice.

We, then, quantified end of the day (EOD) and end of the night (EON) carbon status in the leaves of the two accessions. Glucose and fructose level were significantly lower in *O. australiensis* than *O. sativa* cv. Nipponbare at the EOD and EON (Figure S4a). Sucrose content was marginally, but significantly, higher in *O. australiensis* compared to *O. sativa* cv. Nipponbare at the EOD as well as EON. At the EOD, *O. australiensis* accumulated more starch in leaves than *O. sativa* cv. Nipponbare (Figure S4b). However, *O. australiensis* displayed a significantly lower leaf starch level than *O. sativa* cv. Nipponbare at the EON, suggesting efficient utilization of stored starch in *O. australiensis* during the night (Figure S4b). This is in contrast to lower starch content in the grains of *O. australiensis* as explained earlier (Figure 2c). These results clearly indicated the efficient utilization of the photosynthates in the wild rice, however not towards grain filling, suggesting the possibility of the alternative sink and alternative fate of photosynthates.

Phloem loading and export of sucrose from leaves

Since sucrose is the major transportable form of photosynthates from source leaves to sink organs, we investigated the sucrose transport differences between the two accessions. We performed [^{14}C] labelled sucrose assay in leaf discs of *O. sativa* cv. Nipponbare and *O. australiensis*. The higher amount of ^{14}C per unit leaf disc area was detected *O. australiensis* (5598.83 CPM per cm^2) compared to that of in Nipponbare (3446.66 CPM per cm^2) (Figure 2d). We, then, quantified sucrose in the phloem sap of the two accessions. Phloem sap of *O. australiensis* had four times higher sucrose content than *O. sativa* cv. Nipponbare (Figure 2e). Together, ^{14}C-assay and analysis of phloem sap showed the efficient phloem loading and sucrose export from the leaf in the wild rice *O. australiensis* compared to Nipponbare.

210 **Expression pattern of genes encoding sucrose transporters**

211 We, then, examined the contribution of sucrose transporters for differences in phloem loading
212 and sucrose export from leaves. Transcript levels of genes encoding clade III SWEET transporters, as
213 well as SUT transporters were quantified. Expression analysis of *OsSWEET*s using publicly available
214 datasets showed preferentially source-specific expression of *OsSWEET13* (Figure S5a). *OsSWEET14*
215 also followed a similar source-specific expression pattern, but at a relatively lower expression level than
216 *OsSWEET13*. *OsSWEET15* and *OsSWEET11* showed preferentially sink (panicle and endosperm)-
217 specific expression pattern. The expression levels of *OsSWEET12* was observed to be very low in all
218 the tissues. Consistent with this, quantitative Real Time-PCR results showed higher transcript levels of
219 *OsSWEET13* in flag leaf and stem; *OsSWEET11* in the spikelet; and *OsSWEET15* in the stem, spikelet,
220 and flag leaf of Nipponbare (Figure 3a-d). Interestingly, the transcript level of *OsSWEET13*, encoding
221 preferentially source-specific SWEET transporter, was significantly higher in flag leaf and stem of *O.*
222 *australiensis* compared to Nipponbare (Figure 3a,b). *In silico* expression analysis showed higher
223 expression of *OsSUT1* and *OsSUT2* in different tissue compared to other *OsSUT*s (Figure S5b). qRT-
224 PCR analysis confirmed the generally higher expression of *OsSUT1* and *OsSUT2* in different tissues of
225 Nipponbare (Figure 3e-h). We detected higher transcript levels of *OsSUT1* in the flag leaf, and *OsSUT2*
226 in the stem of *O. australiensis* compared to Nipponbare (Figure 3e,f). The expression pattern of
227 *OsSWEET*s and *OsSUT*s suggested the potential involvement of selected SWEET and SUT transporters,
228 such as OsSWEET13, OsSUT1, and OsSUT2, in efficient phloem loading and sucrose export from leaf
229 to stem in the wild rice.

230 Despite higher photosynthetic efficiency and efficient sucrose transport from source leaves, *O.*
231 *australiensis* produced smaller and lighter grains with less starch content compared to the cultivated
232 variety Nipponbare. Therefore, we also examined the transcript levels of different sucrose transporters
233 in developing spikelets. The expression levels of all the *OsSWEET*s were significantly lower in spikelets
234 of *O. australiensis* compared to Nipponbare, with almost no expression of preferentially sink-specific
235 *OsSWEET15* and *OsSWEET11* (Figure 3d). In addition, the transcript levels of *OsSUT1* was also
236 significantly lower in developing spikelet of *O. australiensis* than Nipponbare (Figure 3h). Thus,
237 reduced grain filling in *O. australiensis* could potentially be associated with reduced expression of
238 *OsSWEET15*, *OsSWEET11*, and *OsSUT1*.

239

240 **Differences in vascular features associated with sucrose transport**

241 Vascular features are also key to photoassimilate partitioning from source to sink tissues.
242 Therefore, we quantified the vein number and vein width in the fully matured flag leaves of the two
243 accessions. *O. australiensis* leaves had more number of wider veins compared to Nipponbare (Figure
244 4a,b). Moreover, *O. australiensis* also exhibited higher vein density with lesser interveinal distance
245 compared to Nipponbare (Figure S6a,b). We, then, checked the organization of vascular bundles at the
246 panicle base of the two accessions, as panicle base is the site of attachment of spikelets to the main plant

247 (Zhang *et al.,* 2002; Zhai *et al.*, 2018). *O. australiensis* had a fewer number of vascular bundles with
248 the reduced area than Nipponbare at the panicle base (Figure 4c,d). We also quantified the vascular
249 features in the stem of the two accessions (Figure 4e,f). Interestingly, we observed ~1.7 times larger
250 vascular bundles in the *O. australiensis* stem compared to Nipponbare. Further, *O. australiensis* stem
251 also had approximately twice the number of vascular bundles than Nipponbare stem due to wider stem
252 (Figure 4f). Taken together, the sucrose might not be efficiently mobilized to panicle in *O. australiensis*,
253 likely due to defects in the vascular bundle at the panicle base and minimal expression of *OsSWEET*s
254 in developing spikelets, strengthening the hypothesis of alternative utilization of photosynthates in the
255 *O. australiensis* stem towards higher biomass.
256
257 **Starch accumulation and expression levels of starch-biosynthesis genes in stem**
258 The leaf photosynthesis, efficient phloem loading in leaves, vascular features as well as the
259 expression pattern of sucrose transporter genes indicated stem to be a major sink organ utilizing sucrose
260 received from leaves in *O. australiensis*. Therefore, we quantified the content of NSCs in stems of the
261 two species at milk-stage of grain filling (Figure 5a, b). Significantly lower amounts of glucose, fructose
262 and sucrose were detected in the stem of *O. australiensis* as compared to Nipponbare (Figure 5a). This
263 was in contrast to more amount of sucrose being exported from leaves of *O. australiensis*. Therefore,
264 we suspected that *O. australiensis* might reserve a high amount of starch in their stem. To our surprise,
265 a negligible amount of starch was present in the stem of *O. australiensis* compared to Nipponbare
266 (Figure 5b). Starch content was, further, found to be very low in the *O. australiensis* stems at different
267 stages and in different internodes (Figure S7a,b). We, then, checked the expression of key genes
268 involved in starch biosynthesis, *OsAPL3*, *OsAPS1* and *OsSSIIb.* Expectedly, very high expressions of
269 these genes were detected in internode and stem of the cultivated variety Nipponbare by both *in silico*
270 expression analysis as well as qRT-PCR analysis (Figure 5c, S8a). Consistent with very low starch
271 levels in *O. australiensis* stem and internode, the transcript abundance of genes encoding two key
272 enzymes, *OsAPL3* and *OsAPS1*, was drastically less in *O. australiensis* compared to Nipponbare
273 (Figure 5c). Lower amount of soluble non-structural carbohydrates, in particular remarkably low starch
274 content, despite efficient sucrose transport from leaves to stem, confirmed an alternative fate to
275 photosynthates in *O. australiensis* stem.
276
277 **Expression levels of sucrose metabolism genes, Sucrose Synthase enzyme activity, and structural**
278 **carbohydrate levels in stem**
279 Invertases (INV) and Sucrose Synthase (SUS) are the key enzymes for degradation of sucrose.
280 Expression of genes encoding Invertases have been shown to be strongly correlated with starch
281 synthesis (Bahaji *et al.*, 2014; Ruan, 2014). Therefore, we checked the expression pattern of different
282 genes encoding cell wall Invertase (*OsCIN1*), cytoplasmic Invertase (*OsNIN7*), and vacuolar Invertase

283 (*OsINV2*) (Figure S9). The expression of *OsCIN1* was drastically lower in *O. australiensis* indicating
284 limited breakdown of sucrose that remained in stem apoplast during the transport.
285 Among all the *OsSUS*s, *OsSUS1* was shown to be highly expressed in internodes (Hirose *et al.*,
286 2008). *In silico* expression analysis also showed high expression of *OsSUS1* in internodes (Figure S8a).
287 Therefore, we checked the intracellular localization of OsSUS1 and expression levels of the
288 corresponding gene. The OsSUS1-YFP signal overlapped with the plasma membrane-localized marker
289 (PM-mCherry), confirming OsSUS1 localization in plasma membrane (Figure S10). *OsSUS1* was
290 expressed four times higher in *O. australiensis* stem than Nipponbare, indicating a possibility of
291 cellulose accumulation in *O. australiensis* stem (Figure 6a). Since SUS catalyzes a reversible cleavage
292 of sucrose, it has a synthesis activity promoting sucrose synthesis and a cleavage activity promoting
293 sucrose degradation. The enzyme activity assay revealed higher OsSUS1 synthesis activity in
294 Nipponbare, while higher cleavage activity in *O. australiensis* (Figure 6b, c). Lesser accumulation of
295 starch, more transcript levels of *OsSUS1*, and higher cleavage activity of OsSUS1 in *O. australiensis*
296 stem compared to Nipponbare along with localization of OsSUS1 to plasma membrane prompted us to
297 check the cellulose content in the stems of the two accessions. Cellulose synthase genes are usually
298 expressed at the highest levels in rice internodes compared to other tissues as evident from *in silico*
299 expression analysis (Figure S8b). Interestingly, transcript levels of *OsCES4*, *OsCES7*, and *OsCES9*,
300 key cellulose synthesis genes, were significantly higher in the stems of *O. australiensis* than in
301 Nipponbare (Figure 6d). Calcofluor-white staining along with cellulose quantification confirmed more
302 cellulose deposition in *O. australiensis* stem compared to Nipponbare (Figure 6e-f). Like cellulose,
303 hemicellulose content was also significantly higher in *O. australiensis* stem compared to Nipponbare
304 (Figure 6f). Taken together, higher expression of *OsSUS1* and higher cleavage activity of OsSUS1
305 coupled with higher expression of Cellulose Synthase genes, at least in part, led to efficient utilization
306 of photosynthates in the *O. australiensis* stem.
307
308

309 **Discussion**

310 We investigated the differences in source-sink dynamics between a cultivated rice variety *O.*
311 *sativa* cv. Nipponbare, which is optimized for high grain yield, and a wild relative of rice *O.*
312 *australiensis*, which accumulates high biomass with poor grain yield. *O. australiensis* had higher source
313 strength, as evident by consistently higher leaf photosynthesis rate compared to Nipponbare, at least in
314 part due to vascular features of the leaf (Figure S3a and 4a-b). High leaf photosynthesis, usually, results
315 in high biomass or yield depending upon preferential sink tissues, provided efficient transport of
316 photoassimilates from leaves (Burnett *et al.*, 2016; Fabre *et al.*, 2020; Fernie *et al.*, 2020). Limitations
317 in sucrose export accumulate sugars in leaves, thereby inhibiting leaf photosynthesis. Therefore, an
318 efficient sucrose export system from leaf would be warranted for the realization of higher source

319 strength of the wild rice to high biomass and/or yield. ^{14}C sucrose uptake assay, as well as sucrose
320 content in phloem sap, confirmed the efficient sucrose export from wild rice leaves (Figure 2 d-e).
321 Larger vascular bundles and fewer number of mesophyll cells between two consecutive veins
322 potentially mediated efficient sucrose export from leaves in wild rice, as reported in different plant
323 system (Qi et al., 2008; Fujita et al., 2013; Mathan et al., 2016). In addition, higher expression of genes
324 encoding sucrose transporters, OsSWEET13 and OsSUT1, would also facilitate the efficient phloem
325 loading in the wild rice (Figure 4). High expression of *SbSWEET8-1* of sorghum, a close homolog of
326 *OsSWEET13*, in leaf and its function in phloem loading supports our idea of the important role of
327 *OsSWEET13* for phloem loading (Mizuno et al. 2016). Similarly, *OsSUT1* not only functions for
328 enhancing phloem loading for sucrose transport but also for retrieval of sucrose from the apoplasm
329 along the transport pathway (Scofield *et al.*, 2007). Higher amount of soluble sugars in wild rice leaves,
330 despite having higher sucrose export from leaves, compared to the cultivated variety, further supported
331 the better source strength of the wild rice (Figure 2 a-b).
332 The better grain filling and higher grain yield of cultivated rice, despite of the relatively lower
333 source strength compared to *O. australiensis*, could be explained by optimal vascular features and
334 desirable expression sucrose transporter genes at the panicle base and spikelets of cultivated rice (Figure
335 3 and 4). Panicle architecture, a key determinant of rice grain yield, is reported to be shaped by the
336 vascular pattern (Sasahara *et al.*, 1999; Terao *et al.*, 2010). Reduced expression of *OsSWEET13* and
337 *OsSWEET15* in the developing spikelet, and of *OsSUT1* at the panicle base and developing spikelet,
338 along with reduced supply of smaller vascular bundles at the panicle base limited mobilization of
339 photosynthates to grains in the wild rice compared to the cultivated. In agreement with this, *ossweet11*
340 *ossweet15* double mutant has been reported to show smaller seed size (Yang *et al.*, 2018). Similarly,
341 RNA antisense lines of *OsSUT1* showed reduced grain filling and grain weight (Scofield *et al.*, 2007).
342 Increased supply of larger vascular bundles to rice rachis has been shown to promote more grains per
343 panicle (Zhang *et al.* 2002; Terao *et al.*, 2010; Zhai *et al.*, 2018). Altogether, higher source strength and
344 limited grain sink strength in the wild rice, attributed to vascular features and sucrose transporter
345 functions, indicated preferential utilization of photosynthates in stem and internodes, contributing to
346 source-sink relationship differences between cultivated and wild rice. In conjunction with this, larger
347 vascular bundles would facilitate efficient sucrose transport and unloading in the wild rice stem. Such
348 vascular feature in the stem would, in turn, also provide mechanical strength to support the high biomass
349 of the wild rice (Aohara *et al.*, 2009). Our expression results indicated the potential involvement of
350 OsSWEET13 and OsSUT2 in unloading larger amount of sucrose being received in the wild stem.
351 There is a competition among the sink tissues for utilization of photosynthates (Patrick *et al.*,
352 2013; Durand *et al.*, 2018). According to EcoMeristem model, the final plant architecture is an outcome
353 of competition for resources among different plant parts that depends on photoassimilate-partitioning
354 patterns (Luquet *et al.*, 2006). More number of longer internodes and thicker stem with larger leaves,
355 driving high biomass in the wild rice compared to the cultivated variety, suggested higher utilization of

356 photosynthates for vegetative growth. The higher biomass and larger organ size of wild rice would
357 require more photosynthates for general respiration and maintenance. However, this would not explain
358 the utilization of photosynthates in total as wild rice showed remarkably higher amount of sucrose in
359 phloem sap compared to the cultivated variety. Altogether, wild rice efficiently utilized
360 photoassimilates reaching to stem towards larger vegetative organ size and number, cell-wall thickening
361 as well as the overall maintenance of higher biomass as compared to the cultivated rice variety.

362 The preferential utilization of photosynthates in the stem/internodes of wild rice in contrast to
363 grains in the cultivated rice suggested differences in the photosynthates metabolism in the stem of the
364 two species. Cultivated rice variety clearly accumulated higher starch content in the stem, which is
365 mobilized to panicle during grain filling (Figure 5b). *OsSWEET11* and *OsSWEET15* have been
366 suggested to be important for remobilization of carbon reserve from stem to grain, and OsSUT1 in the
367 retrieval of sucrose from apoplasmic space to stem for conversion to transitory starch (Wang *et al.*,
368 2020). Indeed, Nipponabre stem showed higher expression of *OsSWEET11*, *OsSWEET15*, and *OsSUT1*
369 compared to the wild rice along with desirable vascular features at the panicle base. High expression of
370 starch biosynthesis genes, further, contributed to the roles of the stem as an effective source in the
371 cultivated variety at the grain filling stage (Figure 7). The differences in the stem starch content between
372 the two genotypes projected the stored transitory starch in the stem as a key for source-sink dynamics
373 favoring high grain yield.

374 *O. australiensis* stem showed higher expression of *OsSUS1* and higher cleavage activity OsSUS
375 producing higher amount of UDP-glucose and fructose compared to cultivated rice. UDP-glucose has
376 been shown to serve as the prime source for cellulose synthesis (Smith *et al*., 2012). UDP-glucose can
377 possibly also be converted to starch (Asano et al., 2002; Koch, 2004). However, the possibility is
378 minimized in the wild rice due to very limited expression of *OsAPL3* and *OsAPS1*. Thus, most of the
379 SUS-generated UDP-glucose was converted to cellulose, supported by high expression of cellulose
380 synthase genes, *OsCES4*, *OsCES7*, and *OsCES9* in the wild stem (Figure 6d-f). OsSUS1 has been
381 reported to be located in SE-CC complexes of phloem, and localization of SUS in phloem is important
382 for cellulose synthesis (Smith *et al*., 2012; Regmi *et al.*, 2016). Plasma membrane localization of
383 OsSUS1 in this study together with earlier reported association of cellulose synthase complexes to
384 plasma membrane highlighted the key importance of OsSUS1 for cellulose synthesis in rice (Figure
385 S10, Lei *et al*., 2012). In addition, SUS functions in companion cells of phloem has been suggested to
386 enhance the sucrose unloading at sink tissues, further helping in unloading photosynthates in wild rice
387 stem (Nolte and Koch, 1993; Stein and Granot, 2019, Yao *et al.*, 2020). The potential role of SUS in
388 cellulose synthesis, as well as in secondary cell wall thickening, has been investigated in past (Coleman
389 *et al.*, 2009; Baroja-Fernández *et al.*, 2012; Wei *et al.*, 2015). Consistent with the higher expression of
390 *OsSUS1* in wild rice, overexpression of *SUS* has been shown to result in increased vegetative growth
391 rate, plant height and biomass in different plant species (Coleman *et al.*, 2006; Nguyen *et al.*, 2016;
392 Stein and Granot, 2019). Contrary to the wild rice, higher synthesis activity of OsSUS in Nipponbare

393 stem would facilitate the formation of sucrose from the stored starch at the heading stage to be mobilized
394 for grain filling. Thus, differential functions in OsSUS1 between wild and cultivated rice would, at least
395 in part, explain the differential fate of photosynthates in the stem (Figure 7).
396 In summary, differences in vascular features and sucrose transporter functions led to a
397 differential source-sink relationship between wild rice *O. australiensis* and cultivated variety *O. sativa*
398 cv. *Nipponbare*. Wild rice showed source-sink dynamics favoring high biomass through accumulation
399 of structural carbohydrates, mediated by higher cleavage activity of SUS enzyme together with higher
400 expression of Cellulose Synthase genes (Figure 7). In contrast, source-sink dynamics favored higher
401 grain yield in Nipponbare via accumulation of transitory starch in the stem, to be mobilized to panicles
402 with the onset of grain filling. Taken together, vascular features and sucrose transporter functions along
403 with transitory starch storage mechanism and SUS enzyme activity can potentially be targeted for
404 source-sink dynamics favoring either biomass accumulation in fodder crops or higher grain yield in
405 cereal crops.
406
407
408 ## Experimental procedures
409 **Phenotyping of the selected rice accessions for biomass and yield-related traits**
410 Two cultivated varieties, *Oryza sativa* ssp. *indica* cv IR 64 and *Oryza sativa* ssp. *japonica* cv
411 Nipponbare, and three wild rice species, *Oryza rufipogon, Oryza latifolia,* and *Oryza australiensis*, were
412 grown in the experimental field of National Institute of Plant Genome Research, New Delhi
413 (*latitude* 28°36 N; *longitude* 77°12 E; *altitude* 216 m) under natural growing conditions. At least ten
414 individual plants for each genotype were phenotyped. Plant architectural traits were quantified at milk-
415 stage of grain-filling. Seed traits and fresh and dry weight were quantified at grain maturity stage. Plant
416 height was measured as the height from the soil surface to the tip of central panicle; total leaves per
417 plant, tiller number per plant, and internode number per the main stem were counted manually; flag leaf
418 width was quantified as the width of the widest portion of the flag leaf, and internode length was
419 calculated using the distance between two consecutive nodes on the main stem. Stem width and
420 circumference were quantified using Fiji-Image J software from images of hand-cut sections of the
421 same region of the main stem. Fresh weight was quantified by directly weighing the entire plant mass,
422 whereas dry weight was quantified by weighing the dried plant mass after drying the entire plant mass
423 at 60°C for five days. Spikelet per panicle was counted manually, whereas seed length and seed width
424 (50 seeds per replicate) were measured using a digital Vernier calliper. For seed weight analysis, 500-
425 seeds were randomly selected and weighed using an electronic balance. Raw data of biomass and grain
426 yield-related traits for each genotype were normalized to median from the entire sample set for principal
427 Component analysis.. Then, all the data were converted on a log base 2 scale on JMP software from
428 SAS (https://www.jmp.com/en_us/home.html).
429

430 **Quantification of leaf photosynthesis rate and related physiological traits**

431 Leaf photosynthesis rate (*A*), stomatal conductance to water (g_sH_2O), and intercellular CO_2
432 concentration (C_i) were recorded from flag leaves at booting, and milk- and dough- stage of grain filling
433 for *O. sativa* ssp. *indica* cv. Nipponbare and *O. australiensis* using a portable photosynthesis system
434 LI-6400XT (LI-COR Biosciences). Data were recorded from at least 15 independent plants of each
435 genotype on a clear day between 9.00 h to 11.00 h under ambient CO_2 level (C_a; 400 µmol mol^{-1}), air
436 temperature (30 ºC), leaf temperature (27 ºC), and photosynthetic photon flux density (PPFD, 1,500
437 µmol m^{-2} s^{-1}) conditions.

438

439 **Quantification of glucose, fructose, and sucrose**

440 The non-structural carbohydrates (NSCs: glucose, fructose, and sucrose) present in the flag leaf and
441 stem were quantified for *O. sativa* ssp. *indica* cv. Nipponbare and *O. australiensis* at the milk-stage of
442 grain-filling by Gas Chromatography-Mass Spectrometry (GC/MS). Flag leaf and stem tissues were
443 harvested from field-grown plants of both the genotypes at 9-11 am. For the quantification of NSCs in
444 flag leaves at the end of the day (EOD) and end of the night, tissue samples were collected at 6.00 pm
445 and 6.00 am, respectively. The tissues were sampled from at least four individual plants per genotypes
446 and immediately frozen into liquid nitrogen after harvesting. A 100 mg fresh weight (FW) of the tissues
447 were extracted using 1.0 ml water: chloroform: methanol (1:1:2.5) spiked with 10 µl internal standard
448 (1 mg ml^{-1} ribitol in water). The mixture was vortexed, centrifuged and 200 µl of polar phase were dried
449 for 3 hours in a Speed-Vac Concentrator. Next, dried samples were derivatized with 50 µl of 20 mg
450 ml^{-1} methoxyamine in pyridine warmed for 37°C for 120 mins with shaking. Metabolites were further
451 derivatized by adding 70 µl of N-methyl N-trimethylsilyl-trifluoroacetamide (MSTFA) at 37°C for 30
452 min. Once derivatization was completed, samples were transferred to GC compatible vials and 1µl of
453 samples were injected on GC-MS-QP2010 (Shimadzu) as described in Lisec *et al.* (2006). For
454 metabolite identification, the mass spectra were matched with commercially available spectral libraries
455 NIST08, NIST11 and Wiley08 for automated peak identification and validated by retention index (RI)
456 libraries (http://gmd.mpimp-golm.mpg.de/). The relative amount of metabolites was presented by total
457 ion current signal which was normalized to Ribitol and tissue weight.

458

459 **Starch quantification**

460 Starch was quantified from flag leaves, stems, matured seeds, and different internodes of *O. sativa* ssp.
461 *indica* cv. Nipponbare and *O. australiensis*. The quantification from flag leaves and stems of the two
462 genotypes were performed at the milk-stage of grain-filling at the time of phenotyping of
463 photosynthesis, whereas flag leaves samples were used for starch quantification at EOD and EON.
464 Starch was also quantified from leaves at vegetative and booting stage, as well as in different internodes
465 of the two species at the milk-stage of grain-filling. Starch was quantified using Mega-Calc Total starch

466 determination kit (K-TSTA; Megazyme) according to the manufacturer's protocol. Four independent
467 biological replicates were analysed for each tissue type for each genotype.
468
469 **^{14}C labelled sucrose loading assay**
470 The phloem loading capacity of ^{14}C labelled sucrose was quantified by following the method as descried
471 by Yadav *et al.* (2017). Briefly, rice flag leaves at milk-stage of grain-filling were cut, and the leaf bases
472 were immediately transferred to petri-dish submerged with MES/$CaCl_2$ buffer (20 mM MES, 2mM
473 CaCl2, pH 5.5 with KOH). Next, leaf discs (3.6 × 1.0 cm) were excised using a cork borer, and
474 immediately placed abaxial side down in the 24-well microtiter plate pre-filled with 1 ml MES/$CaCl_2$
475 buffer spiked with 1mM sucrose solution (1mM unlabelled Sucrose supplemented with 0.81µCi ml^{-1}
476 ^{14}C Sucrose). Leaf discs immersed in the above solution were vacuum-infiltrated for at least 20 min
477 with gentle shaking at room temperature. Labelled leaf discs were transferred to a fresh microtiter plate
478 and washed twice with 1.0 ml MES/$CaCl_2$ buffer, blot dried on absorbent filter paper, and immediately
479 frozen on dry ice and lyophilized. Next, ^{14}C sucrose loading capacity into leaves was quantified by
480 scintillation counting (PerkinElmer). Four leaf discs were used for each biological replicate, and six
481 biological replicates were used for each genotype per experiment.
482
483 **Sucrose quantification in phloem sap**
484 The amount of sucrose in the phloem was quantified using the EDTA-facilitated exudation technique
485 described by King and Zeevaart (1974). Flag leaves of the cultivated and wild rice were excised at the
486 milk-stage of grain-filling at around 9-10 am (when leaf photosynthesis was quantified), leaf bases were
487 immediately recut under exudation buffer (10 mM, Hepes, 10 mM EDTA, pH 7.5) to allow dispersion
488 of any leaf contaminants, and placed in a 15 ml tube containing 5 ml of the exudation buffer. Samples
489 were incubated in a humid chamber (relative humidity >90%) in the dark to prevent evapotranspiration,
490 and exudates were collected after 5 h of incubation. 2 ml of sample aliquots were spiked with 50 µl
491 internal standard (1 mg ml^{-1} ribitol in water), and freeze-dried for sucrose quantification using GC-MS
492 based method as described earlier. Individual flag leaves from different plants were considered as
493 separate biological replicates, and four biological replicates were analyzed for each genotype.
494
495 **RNA isolation, cDNA synthesis and qRT-PCR analysis**
496 Total RNA from flag leaf, stem, and panicle base at milk-stage of grain-filling was extracted using
497 TRIzol reagent (Invitrogen), whereas RNA from spikelet at milk-stage was extracted using plant RNA
498 purification kit (Sigma-Aldrich) according to manufacturer's protocol. One microgram (1µg) of total
499 RNA was reverse transcribed to first strand-cDNA by anchored oligodT priming using Thermo
500 Scientific RevertAid cDNA synthesis kit following manufacturer's instructions. The primer pairs (Table
501 S1) of selected targeted genes used in this study produced a single product as viewed through
502 dissociation curve analysis. Further, the efficiency of each primers was also evaluated using a standard

503 curve method where five cDNA quantities (1, 25, 50, 75, and 100 ng) from each genotype was used to
504 construct a standard curve, and efficiency were calculated using the formula $E = (10^{[-1/slope]}-1)*100$.
505 Expression analysis of each gene was performed at least in three biological replicates for each genotype.
506 The transcript levels of genes were normalized to the stable internal control actin (LOC_Os03g50885),
507 relative expressions of target genes were presented using $2^{-\Delta Ct}$ method by Livak and Schmittgen (2001).
508 *In sillico* expression analysis of the genes was performed using OS_AFFY_RICE_6 dataset present in
509 Genevestigator database (https://genevestigator.com/gv/).
510
511 **Visualization and quantification of anatomical traits**
512 The vascular features of flag leaves as well as vascular bundles in the inner and outer ring of the stem,
513 and panicle base (0.5 cm above the panicle node) were visualized and quantified through hand-cut
514 transverse sections. Flag leaves, stems and panicle bases were hand-sectioned using a razor-blade at the
515 milk-stage of grain-filling, at least from five independent plants for each genotype, and stained with
516 toluidine blue O (0.02% toluidine blue O in water) as described by Mitra and Loqué, (2014).
517 Photographs were taken under a bright field microscope (LMI). Quantification of the different
518 anatomical traits were made using Fiji-Image J software (Wayne Rasband, National Institute of Health).
519
520 **Cellulose staining and quantification**
521 For histochemical visualisation of cellulose, transverse hand-sections of rice stem (approximately 20
522 µm thickness) at the milk-stage of grain-filling were stained using calcofluor white (0.2% calcofluor
523 white M2R in water) staining solution as described by Ambavaram *et al.* (2011). Stained sections were
524 photographed under UV light range using a fluorescence microscope (excitation filter: 340-380 nm;
525 Carl Zeiss Microscopy). The quantification of cellulose and hemicellulose was made using National
526 Renewable Energy Laboratory (NREL) protocols as described in Mund *et al.* (2016). The
527 quantifications were made in four biological replications for each genotype.
528
529 **Estimation of Sucrose synthase synthesis and cleavage activity**
530 The sucrose synthase (SUS) synthesis and cleavage activity were performed in stem tissue of the two
531 genotypes at the milk-stage of grain-filling. Tissue samples were homogenized in extraction buffer (50
532 mM HEPES/NaOH (pH 7.5), 7.5 mM $MgCl_2$, 2 mM EDTA, 2% (w/v) PEG 8000, 2% (w/v) PVP and
533 5 mM DDT) at 4 °C. The homogenate was centrifuged for 1 min at ~16,000 × *g*, the pellet was discarded
534 and the crude extract was used for enzyme assay. To quantify OsSUS synthesis activity, 50 µl of crude
535 extract was incubated with 20 mM HEPES/NaOH buffer (pH 7.5), 5 mM $MgCl_2$, 20 mM KCl, 12 mM
536 fructose, 0.4 mM phosphoenolpyruvate, 2 mM uridine diphosphate UDP-glucose, 20 U pyruvate kinase,
537 20 U lactate dehydrogenase, and 0.15 mM NADH in total 1.0 ml final reaction volume. Similarly, to
538 quantify OsSUS cleavage activity, 50 µl of crude extract was incubated with 20 mM HEPES/NaOH
539 buffer (pH 7.5), 100 mM sucrose, 2 mM UDP, 2mM $MgCl_2$, 0.005 UDP-glucose dehydrogenase, and

540 1.5 mM NAD^+ in total 1.0 ml final reaction volume. The reaction mixture was mixed gently, and
541 decrease and increase in absorbance were recorded for synthesis and cleavage activity, respectively, at
542 340 nm continuously for 0 to 300 sec using a UV–Vis spectrophotometer. The OsSUS activity was
543 calculated in terms of µmol NADH oxidized (synthesis activity) and NAD+ reduced (cleavage activity)
544 per min per mg protein as described in Qazi *et al.* (2012).
545
546 **Subcellular localization of *OsSUS1***
547 Full length of *OsSUS1* CDS without stop codon was cloned under constitutive 35S promoter with a C-
548 terminal eYFP fusion into binary vector pEG10 (Earley *et al.*, 2006). The recombinant plasmid along
549 with empty vector control were then, introduced into EHA105 strain of *Agrobacterium tumefaciens*.
550 Each transformant was co-infiltrated with a plasma membrane-localized marker (PM-mCherry; Nelson
551 *et al.*, 2007) into the leaves of *Nicotiana benthamiana*. Confocal laser scanning microscopy TCS SP5
552 (Leica Microsystems) was used to take the images with appropriate lasers.
553
554 **Accession numbers**
555 Accession numbers of wild rice species used in this study were IRGC 99562, IRGC 99596, and IRGC
556 105272 for *Oryza rufipogon, Oryza latifolia,* and *Oryza australiensis,* respectively.
557
558 **Author Contributions**
559 JM and AR conceptualized the study and designed experiments. JM performed experiments. JM and
560 AS analysed data. JM, AS and AR wrote the manuscript. All the authors have read and edited the final
561 manuscript.
562
563 **Acknowledgements**
564 This work was supported by the Innovative Young Biotechnologist Award (BT/09/IYBA/2015/01) and
565 Ramalingaswamy Re-entry Fellowship (BT/RLF/reentry/05/2013) to AR from the Department of
566 Biotechnology, Ministry of Science and Technology, India. JM and AS acknowledge their CSIR-JRF
567 and SERB-NPDF fellowships, respectively. We also acknowledge Central Instrument Facility, NIPGR;
568 Advanced Instrumentation Research Facility, JNU; Confocal Microscopy Facility, NIPGR; and DBT-
569 eLibrary Consortium (DeLCON) for providing access to e-resources.
570
571 **Conflict of Interest Statement**
572 The authors declare that there is no conflict of interest.
573
574
575

576 **Short legends for Supporting Information**

577 Figure S1. Biomass and yield-related traits of the selected cultivated and wild rice genotypes.

578

579 Figure S2. Principal component analysis of biomass and seed traits of the selected cultivated and wild
580 rice species.

581

582 Figure S3. Leaf photosynthesis and related physiological differences between the cultivated rice *O.*
583 *sativa* cv. Nipponbare and wild rice *O. australiensis*.

584

585 Figure S4. Sugar content in leaves of cultivated rice *O. sativa* cv. Nipponbare and wild rice *O.*
586 *australiensis* at End of Day (EOD) and End of Night (EON).

587

588 Figure S5. *In silico* organ-specific expression analysis of rice genes encoding SWEET and SUT
589 transporters.

590

591 Figure S6. Quantification of leaf interveinal distance and vein density for cultivated rice *O. sativa* cv.
592 Nipponbare and wild rice *O. australiensis*.

593

594 Figure S7. Total starch content in stem and internodes of cultivated rice *O. sativa* cv. Nipponbare and
595 wild rice *O. australiensis*.

596

597 Figure S8. *In silico* expression pattern of key genes involved in sugar metabolism in rice.

598

599 Figure S9. Transcript levels of genes encoding cell wall invertase (*OsCIN1*), cytoplasmic invertase
600 (*OsNIN7*), and vacuolar invertase (*OsINV2*).

601

602 Figure S10. Localization of OsSUS1-YFP in plasma membrane.

603

604 Table S1. List of primer pairs used in the study

605

606

607

608

609

610

611

612

613

References

Ambavaram, M.M.R., Krishnan, A., Trijatmiko, K.R. and Pereira, A. (2011) Coordinated activation of cellulose and repression of lignin biosynthesis pathways in rice. *Plant Physiol.*, **155**, 916–931.

Asano, T., Kunieda, N., Omura, Y., et al. (2002) Rice SPK, a calmodulin-like domain protein kinase, is required for storage product accumulation during seed development: Phosphorylation of sucrose synthase is a possible factor. *Plant Cell*, **14**, 619–628.

Aohara, T., Kotake, T., Kaneko, Y., Takatsuji, H., Tsumuraya, Y. and Kawasaki, S. (2009) Rice brittle culm 5 (brittle node) is involved in secondary cell wall formation in the sclerenchyma tissue of nodes. *Plant Cell Physiol.*, **50**, 1886–1897.

Bahaji, A., Li, J., Sánchez-López, Á.M., et al. (2014) Starch biosynthesis, its regulation and biotechnological approaches to improve crop yields. *Biotechnol. Adv.*, **32**, 87–106.

Baroja-Fernández, E., Muñoz, F.J., Li, J., et al. (2012) Sucrose synthase activity in the sus1/sus2/sus3/sus4 Arabidopsis mutant is sufficient to support normal cellulose and starch production. *Proc. Natl. Acad. Sci. U. S. A.*, **109**, 321–326.

Braun, D.M. (2012) Sweet! The pathway is complete. *Science.*, **335**, 173–174.

Burnett, A.C., Rogers, A., Rees, M. and Osborne, C.P. (2016) Carbon source–sink limitations differ between two species with contrasting growth strategies. *Plant Cell Environ.*, **39**, 2460–2472.

Chen, L.Q., Qu, X.Q., Hou, B.H., Sosso, D., Osorio, S., Fernie, A.R. and Frommer, W.B. (2012) Sucrose efflux mediated by SWEET proteins as a key step for phloem transport. *Science.*, **335**, 207–211.

Cho, J. Il, Kim, H.B., Kim, C.Y., Hahn, T.R. and Jeon, J.S. (2011) Identification and characterization of the duplicate rice sucrose synthase genes OsSUS5 and OsSUS7 which are associated with the plasma membrane. *Mol. Cells*, **31**, 553–561.

Coleman, H.D., Ellis, D.D., Gilbert, M. and Mansfield, S.D. (2006) Up-regulation of sucrose synthase and UDP-glucose pyrophosphorylase impacts plant growth and metabolism. *Plant Biotechnol. J.*, **4**, 87–101.

Coleman, H.D., Yan, J. and Mansfield, S.D. (2009) Sucrose synthase affects carbon partitioning to increase cellulose production and altered cell wall ultrastructure. *Proc. Natl. Acad. Sci. U. S. A.*, **106**, 13118–13123.

Durand, M., Mainson, D., Porcheron, B., Maurousset, L., Lemoine, R. and Pourtau, N. (2018) Carbon source–sink relationship in Arabidopsis thaliana: the role of sucrose transporters. *Planta*, **247**, 587–611.

Earley, K.W., Haag, J.R., Pontes, O., Opper, K., Juehne, T., Song, K. and Pikaard, C.S. (2006) Gateway-compatible vectors for plant functional genomics and proteomics. *Plant J.*, **45**, 616–629.

Fabre, D., Dingkuhn, M., Yin, X., Clément-Vidal, A., Roques, S., Soutiras, A. and Luquet, D. (2020) Genotypic variation in source and sink traits affects the response of photosynthesis and growth to elevated atmospheric CO2. *Plant Cell Environ.*, **43**, 579–593.

Fan, C., Feng, S., Huang, J., et al. (2017) AtCesA8-driven OsSUS3 expression leads to largely enhanced biomass saccharification and lodging resistance by distinctively altering lignocellulose features in rice. *Biotechnol. Biofuels*, **10**, 1–12.

Fernie, A.R., Bachem, C.W.B., Helariutta, Y., et al. (2020) Metabolic Aspects of Source – Sink Interactions. *Nat. Plants*, **6**.

Fujita, D., Trijatmiko, K.R., Tagle, A.G., et al. (2013) NAL1 allele from a rice landrace greatly increases yield in modern indica cultivars. *Proc. Natl. Acad. Sci. U. S. A.*, **110**, 20431–20436.

Guevara, D.R., El-Kereamy, A., Yaish, M.W., Mei-Bi, Y. and Rothstein, S.J. (2014) Functional characterization of the rice UDP-glucose 4-epimerase 1, OsUGE1: A potential role in cell wall carbohydrate partitioning during limiting nitrogen conditions. *PLoS One*, **9**.

Haigler, C.H., Ivanova-Datcheva, M., Hogan, P.S., Salnikov, V. V., Hwang, S., Martin, K. and Delmer, D.P. (2001) Carbon partitioning to cellulose synthesis. *Plant Mol. Biol.*, **47**, 29–51.

Hirose, T., Scofield, G.N. and Terao, T. (2008) An expression analysis profile for the entire sucrose synthase gene family in rice. *Plant Sci.*, **174**, 534–543.

Julius, B.T., Leach, K.A., Tran, T.M., Mertz, R.A. and Braun, D.M. (2017) Sugar transporters in plants: New insights and discoveries. *Plant Cell Physiol.*, **58**, 1442–1460.

King, R.W. and Zeevaart, J.A.D. (1974) Enhancement of Phloem Exudation from Cut Petioles by

669 Chelating Agents. *Plant Physiol.*, **53**, 96–103.
670 **Koch, K.** (2004) Sucrose metabolism: Regulatory mechanisms and pivotal roles in sugar sensing and
671 plant development. *Curr. Opin. Plant Biol.*, **7**, 235–246.
672 **Lei, L., Li, S., and Gu, Y.** (2012). Cellulose synthase complexes: composition and regulation.
673 *Frontiers in plant science*, **3**, 75.
674 **Lisec, J., Schauer, N., Kopka, J., Willmitzer, L. and Fernie, A.R.** (2006) Gas chromatography mass
675 spectrometry-based metabolite profiling in plants. *Nat. Protoc.*, **1**, 387–396.
676 **Livak, K.J. and Schmittgen, T.D.** (2001) Analysis of relative gene expression data using real-time
677 quantitative PCR and the 2-ΔΔCT method. *Methods*, **25**, 402–408.
678 **Luquet, D., Dingkuhn, M., Kim, H., Tambour, L. and Clement-Vidal, A.** (2006) EcoMeristem, a
679 model of morphogenesis and competition among sinks in rice. 1. Concept, validation and
680 sensitivity analysis. *Funct. Plant Biol.*, **33**, 309–323.
681 **Mathan, J., Bhattacharya, J. and Ranjan, A.** (2016) Enhancing crop yield by optimizing plant
682 developmental features. *Dev.*, **143**.
683 **Mitra, P.P. and Loqué, D.** (2014) Histochemical staining of Arabidopsis thaliana secondary cell wall
684 elements. *J. Vis. Exp.,* **13**, 51381.
685 **Mizuno, H., Kasuga, S. and Kawahigashi, H.** (2016) The sorghum *SWEET* gene family: stem
686 sucrose accumulation as revealed through transcriptome profiling. *Biotechnol Biofuels*, **9,** 127
687 (2016).
688 **Mund, N.K., Dash, D., Barik, C.R., Goud, V. V., Sahoo, L., Mishra, P. and Nayak, N.R.** (2016)
689 Chemical composition, pretreatments and saccharification of Senna siamea (Lam.) H.S. Irwin &
690 Barneby: An efficient biomass producing tree legume. *Bioresour. Technol.*, **207**, 205–212.
691 **Nelson, B.K., Cai, X. and Nebenführ, A.** (2007) A multicolored set of in vivo organelle markers for
692 co-localization studies in Arabidopsis and other plants. *Plant J.*, **51**, 1126–1136.
693 **Nguyen, Q.A., Luan, S., Wi, S.G., Bae, H., Lee, D.S. and Bae, H.J.** (2016) Pronounced phenotypic
694 changes in transgenic tobacco plants overexpressing sucrose synthase may reveal a novel sugar
695 signaling pathway. *Front. Plant Sci.*, **6**, 1216.
696 **Nolte, K.D. and Koch, K.E.** (1993) Companion-cell specific localization of sucrose synthase in zones
697 of phloem loading and unloading. *Plant Physiol.*, **101**, 899–905.
698 **Osorio, S., Ruan, Y.L. and Fernie, A.R.** (2014) An update on source-to-sink carbon partitioning in
699 tomato. *Front. Plant Sci.*, **5**, 1–11.
700 **Patrick, J.W., Botha, F.C. and Birch, R.G.** (2013) Metabolic engineering of sugars and simple sugar
701 derivatives in plants. *Plant Biotechnol. J.*, **11**, 142–156.
702 **Qazi, H.A., Paranjpe, S. and Bhargava, S.** (2012) Stem sugar accumulation in sweet sorghum -
703 Activity and expression of sucrose metabolizing enzymes and sucrose transporters. *J. Plant*
704 *Physiol.*, **169**, 605–613.
705 **Qi, J., Qian, Q., Bu, Q., et al.** (2008) Mutation of the rice narrow leaf1 gene, which encodes a novel
706 protein, affects vein patterning and polar auxin transport. *Plant Physiol.*, **147**, 1947–1959.
707 **Regmi, K.C., Zhang, S. and Gaxiola, R.A.** (2016) Apoplasmic loading in the rice phloem supported
708 by the presence of sucrose synthase and plasma membrane-localized proton pyrophosphatase.
709 *Ann. Bot.*, **117**, 257–268.
710 **Ruan, Y.-L.** (2014) Sucrose Metabolism: Gateway to Diverse Carbon Use and Sugar Signaling. *Annu.*
711 *Rev. Plant Biol.*, **65**, 33–67.
712 **Sack, L. and Scoffoni, C.** (2013) Leaf venation: structure, function, development, evolution, ecology
713 and applications in the past, present and future. *New Phytol.*, **198**, 983–1000.
714 **Sanchez, P.L., Wing, R.A. and Brar, D.S.** (2013) The wild relative of rice: genomes and genomics.
715 In *Genetics and genomics of rice* (Zhang, Q. and Wing, R.A., eds). Springer, pp. 10–25.
716 **Sasahara, H., Fukuta, Y. and Fukuyama, T.** (1999) Mapping of QTLs for Vascular Bundle System
717 and Spike Morphology in Rice, *Oryza satva* L. *Breed. Sci.*, **49**, 75–81.
718 **Scofield, G.N., Hirose, T., Aoki, N. and Furbank, R.T.** (2007) Involvement of the sucrose transporter,
719 OsSUT1, in the long-distance pathway for assimilate transport in rice. *J. Exp. Bot.*, **58**, 3155–
720 3169.
721 **Scofield, G.N., Hirose, T., Gaudron, J.A., Upadhyaya, N.M., Ohsugi, R. and Furbank, R.T.** (2002)
722 Antisense suppression of the rice sucrose transporter gene, OsSUT1, leads to impaired grain filling

723 and germination but does not affect photosynthesis. *Funct. Plant Biol.*, **29**, 815–826.
724 **Smith, A.M., Kruger, N.J. and Lunn, J.E.** (2012) Source of sugar nucleotides for starch and cellulose
725 synthesis. *Proc. Natl. Acad. Sci. U. S. A.*, **109**, E776–E776.
726 **Smith, A.M. and Stitt, M.** (2007) Coordination of carbon supply and plant growth. *Plant, Cell*
727 *Environ.*, **30**, 1126–1149.
728 **Smith, M.R., Rao, I.M. and Merchant, A.** (2018) Source-sink relationships in crop plants and their
729 influence on yield development and nutritional quality. *Front. Plant Sci.*, **871**, 1–10.
730 **Stein, O. and Granot, D.** (2019) An overview of sucrose synthases in plants. *Front. Plant Sci.*, **10**, 1–
731 14.
732 **Tanaka, K., Murata, K., Yamazaki, M., Onosato, K., Miyao, A. and Hirochika, H.** (2003) Three
733 distinct rice cellulose synthase catalytic subunit genes required for cellulose synthesis in the
734 secondary wall. *Plant Physiol.*, **133**, 73–83.
735 **Terao, T., Nagata, K., Morino, K. and Hirose, T.** (2010) A gene controlling the number of primary
736 rachis branches also controls the vascular bundle formation and hence is responsible to increase
737 the harvest index and grain yield in rice. *Theor. Appl. Genet.*, **120**, 875–893.
738 **Wang, D., Qin, Y., Fang, J., Yuan, S., Peng, L., Zhao, J. and Li, X.** (2016) A missense mutation in
739 the zinc finger domain of OsCESA7 deleteriously affects cellulose biosynthesis and plant growth
740 in rice. *PLoS One*, **11**, 1–16.
741 **Wang, D.R., Han, R., Wolfrum, E.J. and McCouch, S.R.** (2017) The buffering capacity of stems:
742 genetic architecture of nonstructural carbohydrates in cultivated Asian rice, Oryza sativa. *New*
743 *Phytol.*, **215**, 658–671.
744 **Wang, G., Li, H., Gong, Y., Yang, J., Yi, Y., Zhang, J. and Ye, N.** (2020) Expression profile of the
745 carbon reserve remobilization from the source to sink in rice in response to soil drying during
746 grain filling. *Food Energy Secur.*, 1–14.
747 **Wei, Z., Qu, Z., Zhang, L., Zhao, S., Bi, Z., Ji, X., Wang, X. and Wei, H.** (2015) Overexpression of
748 poplar xylem sucrose synthase in tobacco leads to a thickened cell wall and increased height. *PLoS*
749 *One*, **10**, 1–20.
750 **White, A.C., Rogers, A., Rees, M. and Osborne, C.P.** (2016) How can we make plants grow faster?
751 A source-sink perspective on growth rate. *J. Exp. Bot.*, **67**, 31–45.
752 **Yadav, U., Khadilkar, A., Shaikh, M., Turgeon, R. and Ayre, B.** (2017) Quantifying the Capacity
753 of Phloem Loading in Leaf Disks with [14C]Sucrose. *Bio-Protocol*, **7**, 1–12.
754 **Yang, J., Luo, D., Yang, B., Frommer, W.B. and Eom, J.S.** (2018) SWEET11 and 15 as key players
755 in seed filling in rice. *New Phytol.*, **218**, 604–615.
756 **Yao, D., Gonzales-Vigil, E. and Mansfield, S.D.** (2020) Arabidopsis sucrose synthase localization
757 indicates a primary role in sucrose translocation in phloem. *J. Exp. Bot.*, **71**, 1858–1869.
758 **Zhai, L., Zheng, T., Wang, X., Wang, Y., Chen, K., Wang, S., Wang, Y., Xu, J. and Li, Z.** (2018)
759 QTL mapping and candidate gene analysis of peduncle vascular bundle related traits in rice by
760 genome-wide association study. *Rice*, **11**.
761 **Zhang ZH, Li P, Wang LX, Tan CJ, Hu ZL, Zhu YG, Zhu LH** (2002) Identification of
762 quantitative trait loci (QTLs) for the characters of vascular bundles in peduncle related to indica -
763 japonica differentiation in rice (*Oryza sativa L.*) *Euphytica*, **128**, 279 –284.
764
765
766
767
768
769
770
771

Figure legends

Figure 1. Comparison of biomass and yield-related traits of the selected cultivated and wild rice genotypes.

(a) Shown are the photographs of the selected rice genotypes at the reproductive stage (scale bar = 30 cm).

(b – i) Quantification of plant height (b), total leaves per plant (c), flag leaf width (d), total internode number per main stem (e), fresh weight (f), dry weight (g), spikelet per panicle (h), and 500-seed weight (i) of the selected rice genotypes. Significance of difference among the genotypes was calculated using One-Way ANOVA with Tukey's post-hoc test (n = 10 data point from different plants, $p < 0.05$).

Figure 2. Sugar accumulation, phloem loading, and sucrose export from a leaf for the cultivated rice *O. sativa* cv. Nipponbare and wild rice *O. australiensis*.

(a) Shown are glucose, fructose and sucrose content in the flag leaves of the cultivated and wild rice at the time of photosynthesis quantification.

(b – c) Starch content in the flag leaves (b), and in the matured seeds (c) of the cultivated and wild rice.

(d) Uptake of [^{14}C] sucrose in the flag leaf discs of the two species expressed as counts per minute per square centimeter of leaf area.

(e) Sucrose quantification in the phloem sap of the two species.

Data represents the mean and standard error of mean (SE), and significance of difference between the genotype was calculated using student t-test (*$p < 0.05$, **$p < 0.01$, ***$p < 0.001$).

Figure 3. Tissue-specific expression pattern of genes encoding SWEET and SUT transporters in cultivated rice *O. sativa* cv. Nipponbare and wild rice *O. australiensis*.

(a – d) Transcript levels of *SWEET* genes in the flag leaf (a), stem (b) panicle base (c), and spikelet (d) at the milk-stage of grain-filling in the two rice species.

(e – h) Transcript levels of *SUT* genes in the flag leaf (e), stem (f) panicle base (g), and spikelet (h) at the milk-stage of grain-filling in the two rice species.

Data represents the mean and standard error of mean (SE) from three biological replicate per genotype (n = 3). Significance of difference between the genotype was calculated using student t-test (*$p < 0.05$, **$p < 0.01$, ***$p < 0.001$).

Figure 4. Vascular features in flag leaf, panicle base, and stem of cultivated rice *O. sativa* cv. Nipponbare and wild rice *O. australiensis*.

(a -b) Cross-sections of flag leaves of the two species (a, scale bar = 100 μm), and quantification of minor vein width and the total number of veins (b).

(c - d) Transverse sections at the panicle base (0.5 cm above panicle node) of the two species (c, scale bar = 250 μm), and quantifcation of number and area of vascular bundles (d).

809 (e - f) Transverse sections of stems of the two species (e, scale bar = 100 µm), and quantification of
810 number and area of vascular bundles (f).
811 The peripheral concentric ring of the panicle base and stem is represented as outer ring, and the inner
812 wider circle is represented as inner ring in figures.
813 Data represents the mean and standard error of mean (SE) from fifteen cross-section images collected
814 from five different plants and significance difference between the genotype was based on student t-test
815 (*$p < 0.05$, **$p < 0.01$, ***$p < 0.001$).
816
817 **Figure 5.** Quantification of soluble sugars and expression pattern of starch-biosynthesis genes in stems
818 of cultivated rice *O. sativa* cv. Nipponbare and wild rice *O. australiensis* at milk-stage of grain-filling.
819 (a-b) Glucose, fructose, and sucrose content (a), and total starch content (b) in the stem of the two
820 species (n = 4).
821 (c) Transcript levels of starch-biosynthesis genes, *OsAPL3* (encoding ADP-glucose pyrophosphorylase
822 large subunit), *OsAPS1* (encoding ADP-glucose pyrophosphorylase small subunit), and *OsSSIIB*
823 (encoding Starch synthase), in the stem of the two species.
824 Data represents the mean and standard error of mean (SE), and significance difference between the
825 genotype was calculated using student t-test (*$p < 0.05$, **$p < 0.01$, ***$p < 0.001$).
826
827 **Figure 6.** Expression levels of sucrose metabolism genes, Sucrose Synthase enzyme activity, and
828 structural carbohydrates levels in stem tissue of cultivated rice *O. sativa* cv. Nipponbare and wild rice
829 *O. australiensis* at milk-stage of grain-filling.
830 (a) Transcript levels of *Sucrose Synthase* 1 (*OsSUS1*).
831 (b-c) Enzyme activity of OsSUS in synthesis (b) and cleavage (c) direction.
832 (d) Transcript levels of *Cellulose Synthase* genes, *OsCES4*, *OsCES7*, and *OsCES9*.
833 (e) Calcofluor-white staining for cellulose deposition in the transverse stem sections of the two species.
834 Red arrowhead shows higher deposition of cellulose in *O. australiensis* stem. Scale bar represents 500
835 µm.
836 (f) Quantification of cellulose and hemicellulose in the stems of the two species.
837 Data in a- d and f represents the mean and standard error of mean (SE), and significance of difference
838 between the genotype was calculated using student t-test (*$p < 0.05$, **$p < 0.01$, ***$p < 0.001$).
839
840 **Figure 7.** A model explaining the contribution of sucrose transport, Sucrose Synthase activity, starch
841 biosynthesis, and synthesis of structural carbohydrates towards yield and biomass differences between
842 wild rice *O. australiensis* and cultivated rice *O. sativa* cv. Nipponbare.
843 High leaf photosynthesis rate coupled with higher expression of selected *OsSWEET* and *OsSUT* genes
844 lead to efficient export of sucrose from leaf in *O. australiensis* compared to *O. sativa* cv. Nipponbare.
845 Sucrose, after getting unloaded to stem due to functions of *OsSWEET13*, *OsSUT1*, and *OsSUT2*, gets

converted to UDP-G more efficiently in the wild rice due to higher expression of *OsSUS1* and more cleavage activity of OsSUS compared to the cultivated rice. Higher expression of *OsCES4, OsCES7,* and *OsCES9*, then, leads to more synthesis of cellulose in the stem of the wild rice. In contrast, higher expression of starch-biosynthesis genes, *AGPase* (small and large subunit), leads to higher starch content in the stem of the cultivated rice. Higher synthesis activity of OsSUS along with more expression of *OsSWEET11* and *OsSWEET15* in the cultivated rice facilitate efficient remobilisation of sucrose from stem to panicles at the grain-filling stage. SUC, sucrose (yellow colour circle); F, fructose; G, glucose; UDP-G, UDP-glucose; ADP-G, ADP-glucose; *INV*, Invertase; cwINV, cell wall Invertase; SUS, Sucrose Synthase.

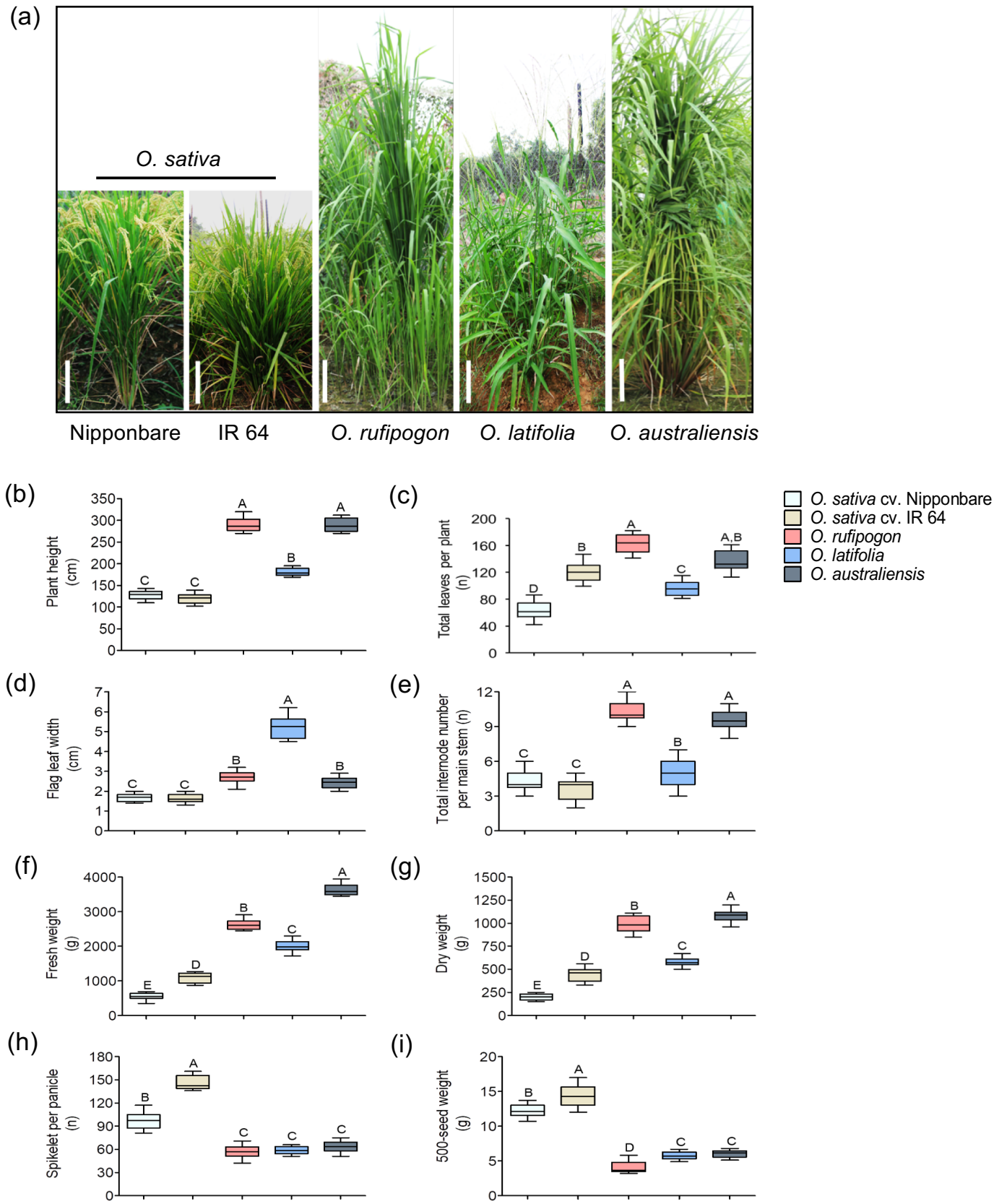

Figure 1. Comparison of biomass and yield-related traits of the selected cultivated and wild rice genotypes.
(a) Shown are the photographs of the selected rice genotypes at the reproductive stage (scale bar = 30 cm).
(b – i) Quantification of plant height (b), total leaves per plant (c), flag leaf width (d), total internode number per main stem (e), fresh weight (f), dry weight (g), spikelet per panicle (h), and 500-seed weight (i) of the selected rice genotypes. Significance of difference among the genotypes was calculated using One-Way ANOVA with Tukey's post-hoc test (n = 10 data point from different plants, $p < 0.05$).

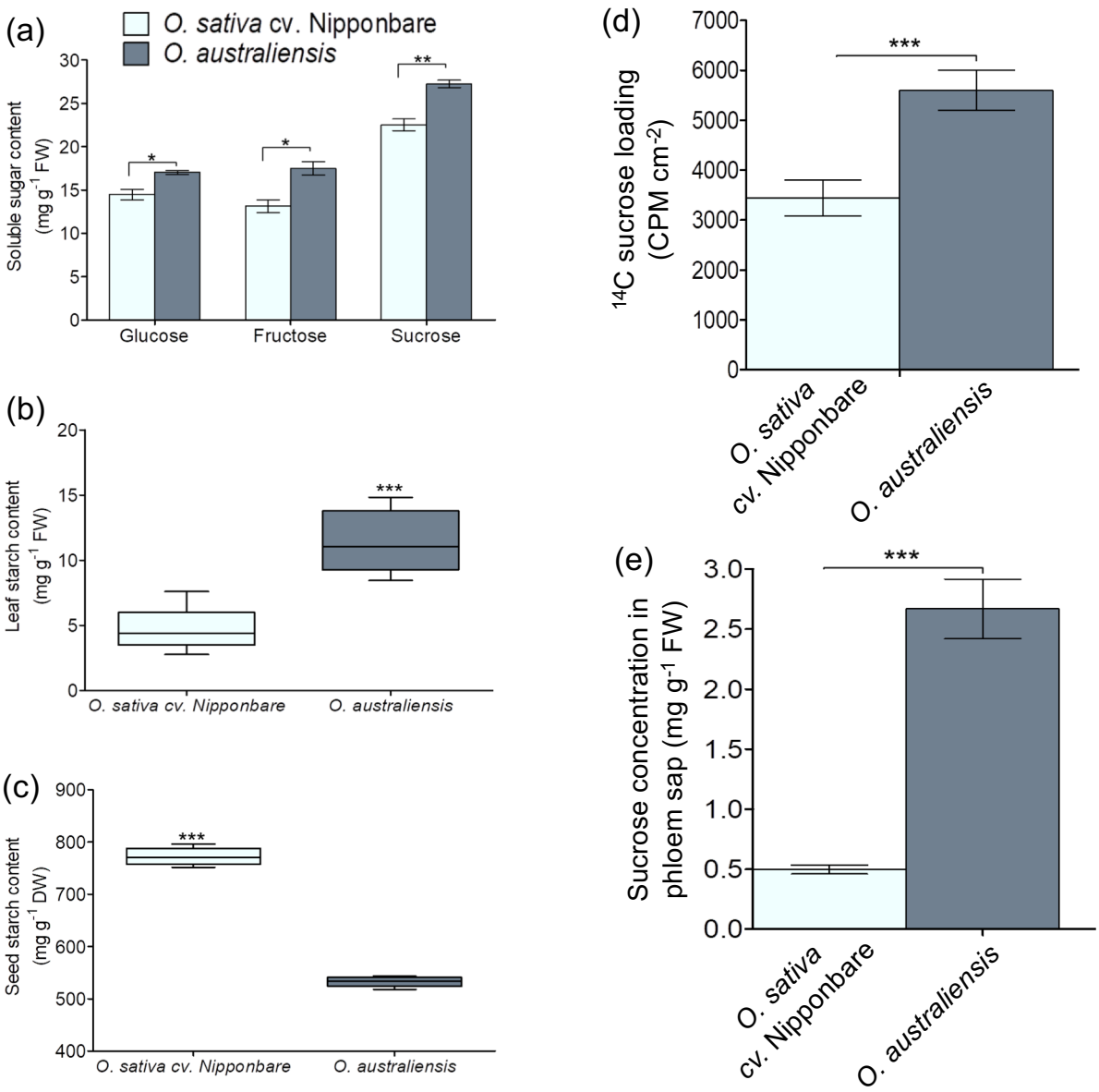

Figure 2. Sugar accumulation, phloem loading, and sucrose export from a leaf for the cultivated rice *O. sativa* cv. Nipponbare and wild rice *O. australiensis*.

(a) Shown are glucose, fructose and sucrose content in the flag leaves of the cultivated and wild rice at the time of photosynthesis quantification.

(b – c) Starch content in the flag leaves (b), and in the matured seeds (c) of the cultivated and wild rice.

(d) Uptake of [^{14}C] sucrose in the flag leaf discs of the two species expressed as counts per minute per square centimeter of leaf area.

(e) Sucrose quantification in the phloem sap of the two species.

Data represents the mean and standard error of mean (SE), and significance of difference between the genotype was calculated using student t-test (*$p < 0.05$, **$p < 0.01$, ***$p < 0.001$).

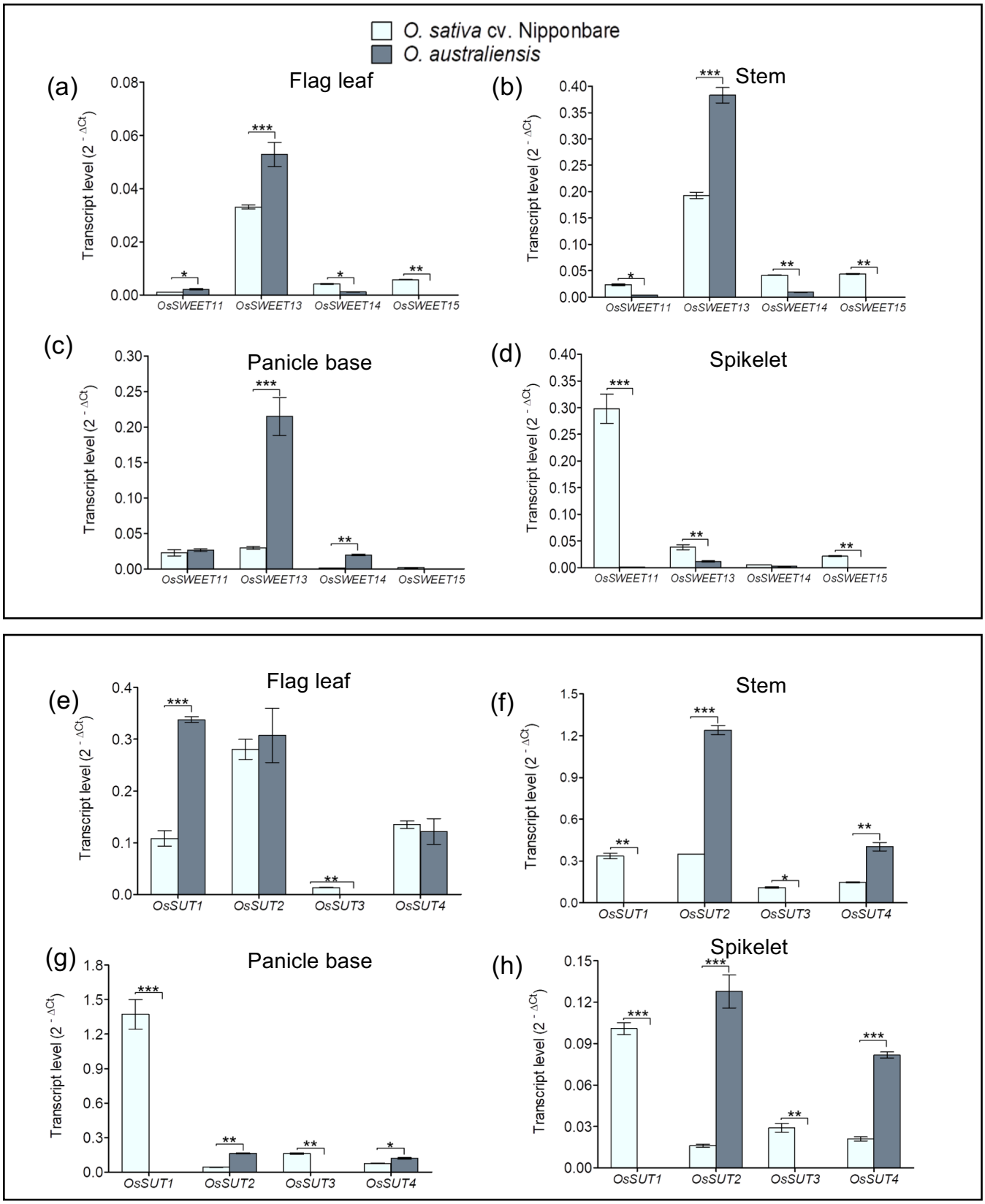

Figure 3. Tissue-specific expression pattern of genes encoding SWEET and SUT transporters in cultivated rice *O. sativa* cv. Nipponbare and wild rice *O. australiensis*.

(a – d) Transcript levels of *SWEET* genes in the flag leaf (a), stem (b) panicle base (c), and spikelet (d) at the milk-stage of grain-filling in the two rice species.

(e – h) Transcript levels of *SUT* genes in the flag leaf (e), stem (f) panicle base (g), and spikelet (h) at the milk-stage of grain-filling in the two rice species.

Data represents the mean and standard error of mean (SE) from three biological replicate per genotype (n = 3). Significance of difference between the genotype was calculated using student t-test (*p < 0.05, **p < 0.01, ***p < 0.001).

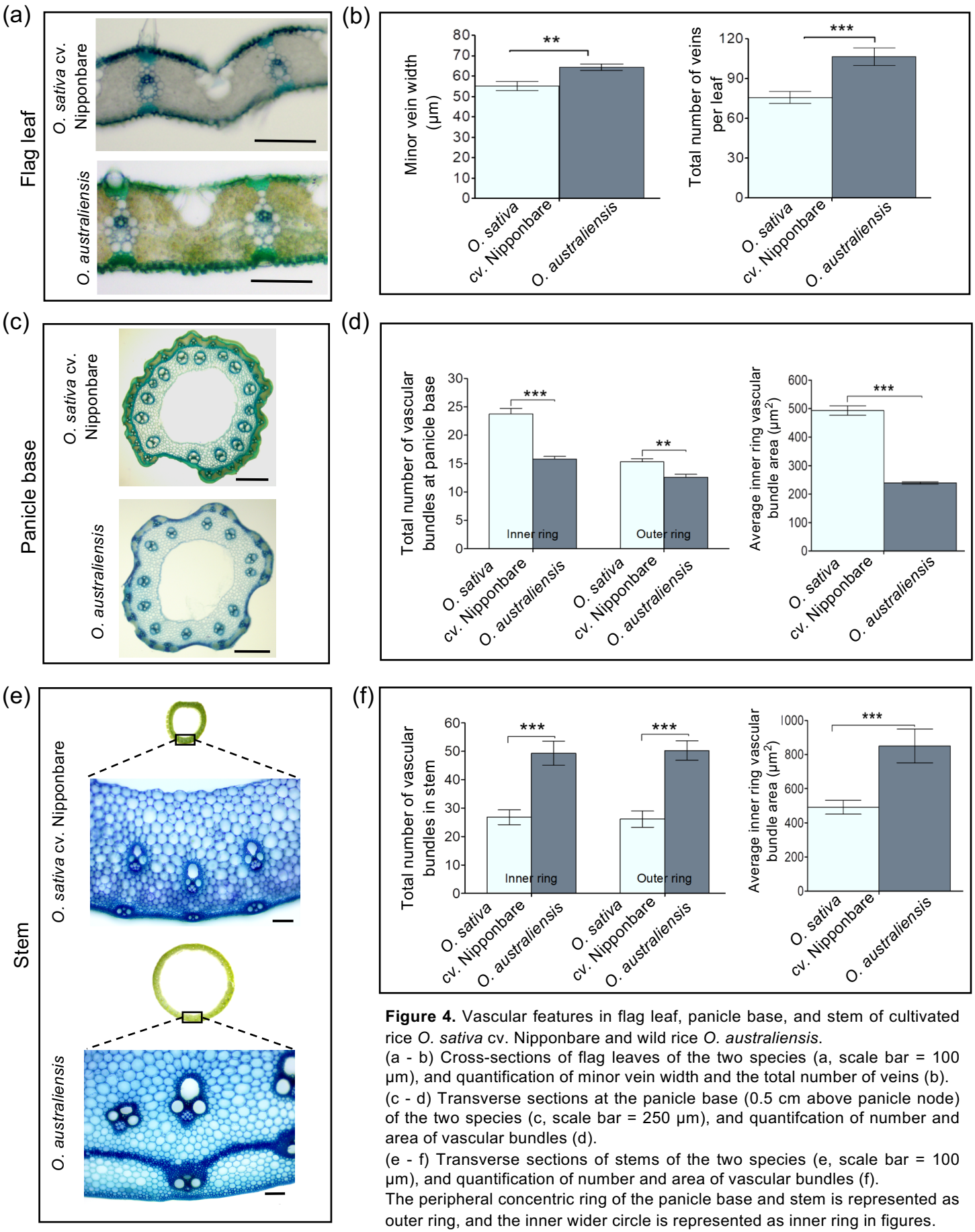

Figure 4. Vascular features in flag leaf, panicle base, and stem of cultivated rice *O. sativa* cv. Nipponbare and wild rice *O. australiensis*.
(a - b) Cross-sections of flag leaves of the two species (a, scale bar = 100 μm), and quantification of minor vein width and the total number of veins (b).
(c - d) Transverse sections at the panicle base (0.5 cm above panicle node) of the two species (c, scale bar = 250 μm), and quantifcation of number and area of vascular bundles (d).
(e - f) Transverse sections of stems of the two species (e, scale bar = 100 μm), and quantification of number and area of vascular bundles (f).
The peripheral concentric ring of the panicle base and stem is represented as outer ring, and the inner wider circle is represented as inner ring in figures.
Data represents the mean and standard error of mean (SE) from fifteen cross-section images collected from five different plants and significance difference between the genotype was based on student t-test (*$p < 0.05$, **$p < 0.01$, ***$p < 0.001$).

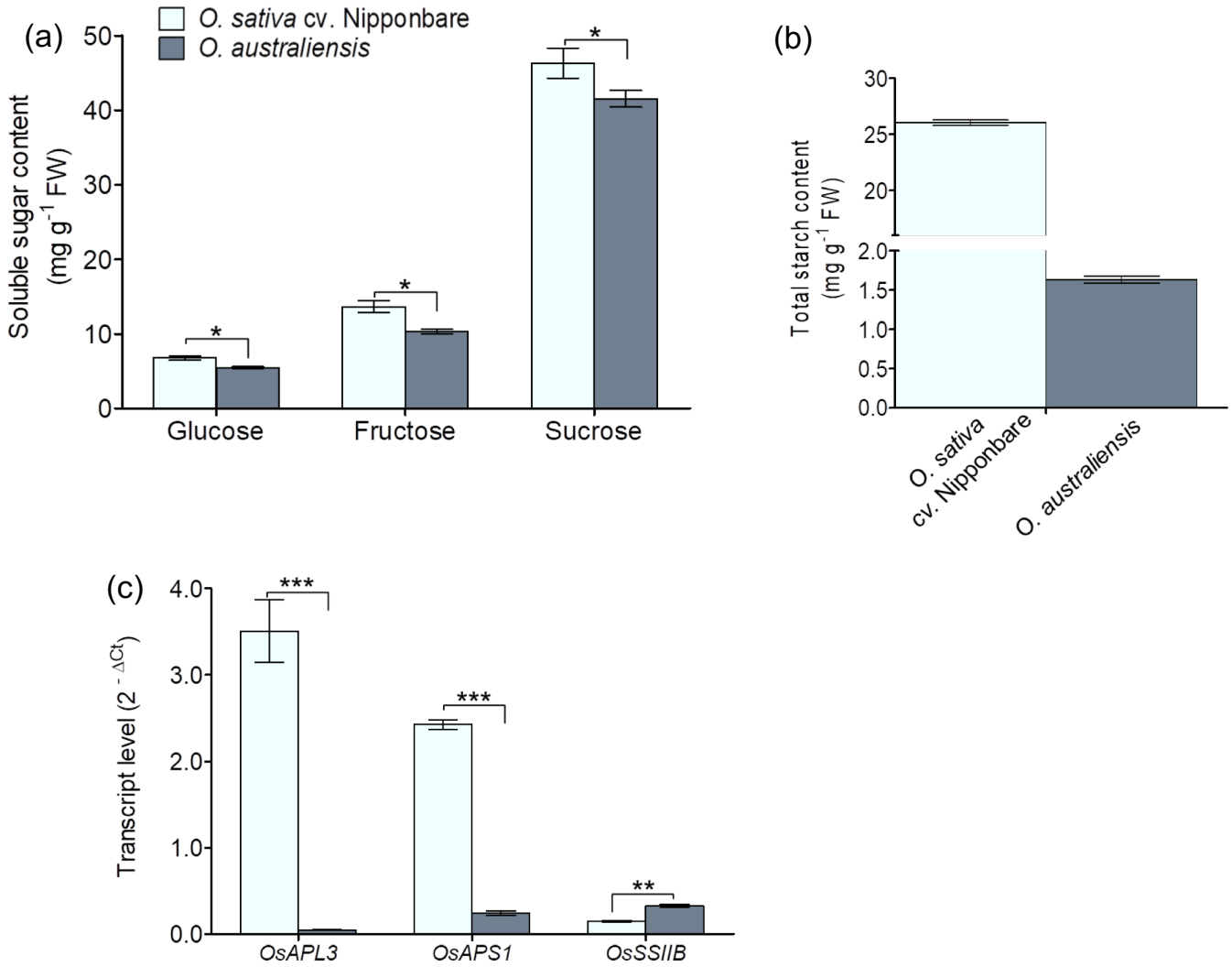

Figure 5. Quantification of soluble sugars and expression pattern of starch-biosynthesis genes in stems of cultivated rice *O. sativa* cv. Nipponbare and wild rice *O. australiensis* at milk-stage of grain-filling.
(a-b) Glucose, fructose, and sucrose content (a), and total starch content (b) in the stem of the two species (n = 4).
(c) Transcript levels of starch-biosynthesis genes, *OsAPL3* (encoding ADP-glucose pyrophosphorylase large subunit), *OsAPS1* (encoding ADP-glucose pyrophosphorylase small subunit), and *OsSSIIB* (encoding Starch synthase), in the stem of the two species.
Data represents the mean and standard error of mean (SE), and significance difference between the genotype was calculated using student t-test (*$p < 0.05$, **$p < 0.01$, ***$p < 0.001$).

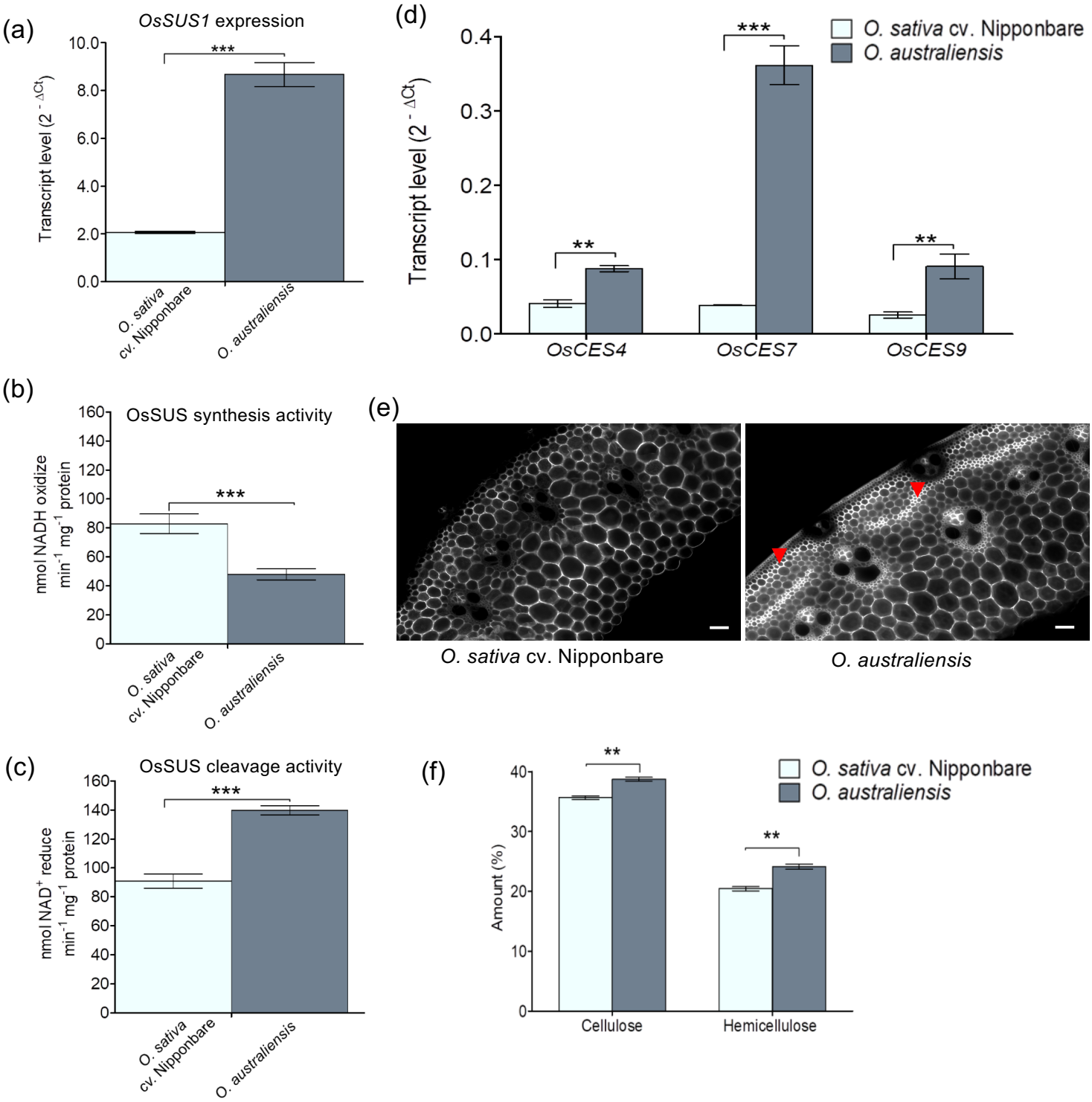

Figure 6. Expression levels of sucrose metabolism genes, Sucrose Synthase enzyme activity, and structural carbohydrates levels in stem tissue of cultivated rice *O. sativa* cv. Nipponbare and wild rice *O. australiensis* at milk-stage of grain-filling.

(a) Transcript levels of *Sucrose Synthase* 1 (*OsSUS1*).

(b-c) OsSUS enzyme activity in synthesis (b) and cleavage (c) direction.

(d) Transcript levels of *Cellulose Synthase* genes, *OsCES4*, *OsCES7*, and *OsCES9*.

(e) Calcofluor-white staining for cellulose deposition in the transverse stem sections of the two species. Red arrowhead shows higher deposition of cellulose in *O. australiensis* stem. Scale bar represents 500 µm.

(f) Quantification of cellulose and hemicellulose in the stems of the two species.

Data in a- d and f represents the mean and standard error of mean (SE), and significance of difference between the genotype was calculated using student t-test (*$p < 0.05$, **$p < 0.01$, ***$p < 0.001$).

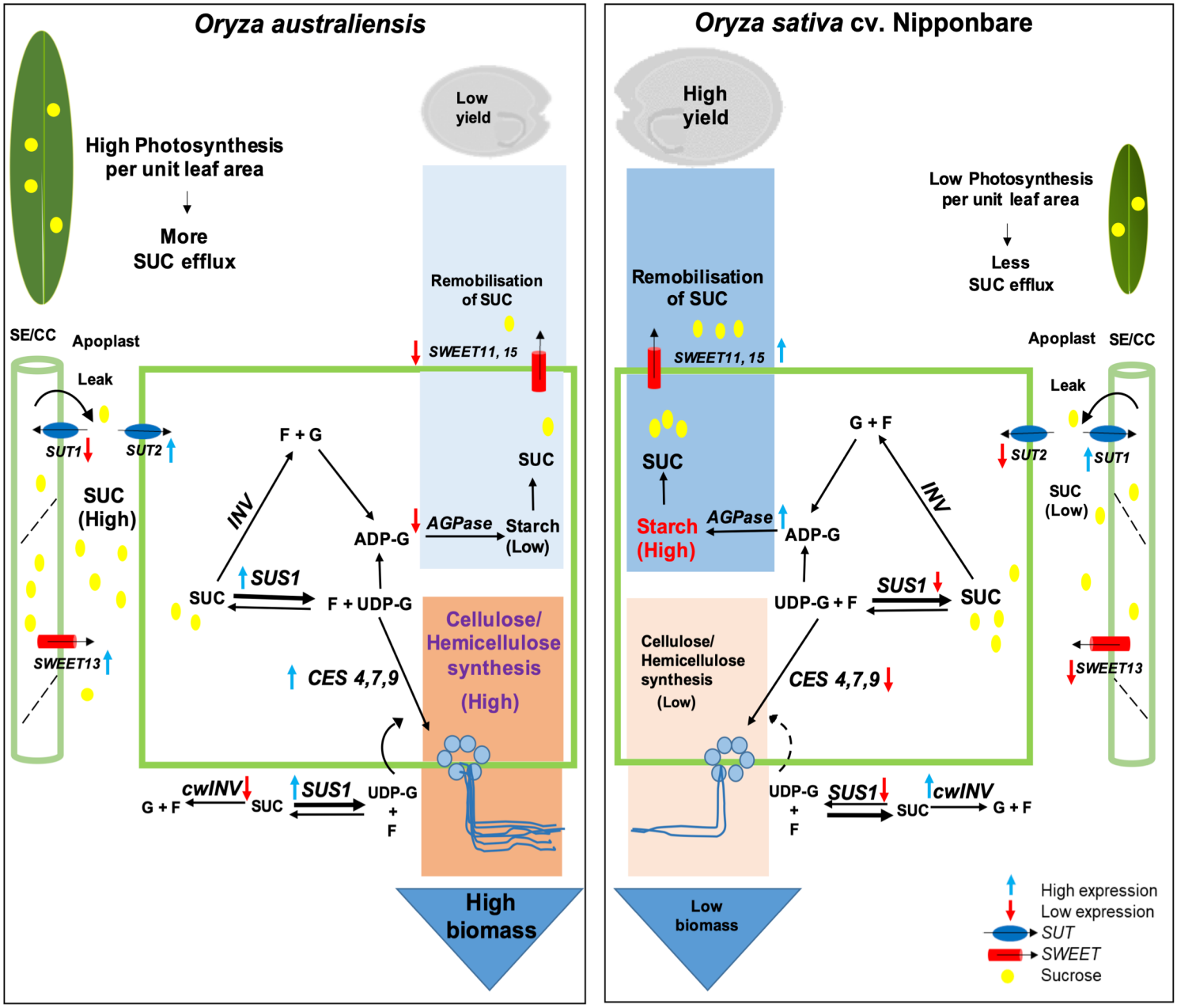

Figure 7. A model explaining the contribution of sucrose transport, Sucrose Synthase activity, starch biosynthesis, and synthesis of structural carbohydrates towards yield and biomass differences between wild rice *O. australiensis* and cultivated rice *O. sativa* cv. Nipponbare.

High leaf photosynthesis rate coupled with higher expression of selected *OsSWEET* and *OsSUT* genes lead to efficient export of sucrose from leaf in *O. australiensis* compared to *O. sativa* cv. Nipponbare. Sucrose, after getting unloaded to stem due to functions of *OsSWEET13*, *OsSUT1*, and *OsSUT2*, gets converted to UDP-G more efficiently in the wild rice due to higher expression of *OsSUS1* and more cleavage activity of OsSUS compared to the cultivated rice. Higher expression of *OsCES4, OsCES7,*and *OsCES9*, then, leads to more synthesis of cellulose in the stem of the wild rice. In contrast, higher expression of starch-biosynthesis genes, *AGPase* (small and large subunit), leads to higher starch content in the stem of the cultivated rice. Higher synthesis activity of OsSUS along with more expression of *OsSWEET11* and *OsSWEET15* in the cultivated rice facilitate efficient remobilisation of sucrose from stem to panicles at the grain-filling stage. SUC, sucrose (yellow colour circle); F, fructose; G, glucose; UDP-G, UDP-glucose; ADP-G, ADP-glucose; *INV*, Invertase; cwINV, cell wall Invertase; SUS, Sucrose Synthase.